Bearing Capacity Analyses of Shallow Foundations in Reinforced Slopes

Kim, Hong-Taek*[1]

Choi, In-Sik*[2]

Sim, Young-Jong*[3]

요 지

최근에 들어 사면이나 사면 근처에 교대등과 같이 기초하중이 비교적 큰 구조물들이 시공되는 예가 점차 많아지는 경향을 보이고 있다. 그러나 일반적으로 사면 또는 사면 근처에 설치되는 기초의 경우는 수평지반에 비해 지지력이 현저하게 떨어지기 때문에, 말뚝이나 케이슨 등과 같은 고가의 깊은기초들이 주로 사용되고 있는 실정이다. 따라서 토목섬유 또는 metal strip 등의 보강재를 이용하여 사면을 보강하는 경제적인 공법이 필요시 되고, 또한 이와같은 공법에 관련된 합리적인 기초지지력 해석법의 제시가 요구되고 있다. 본 연구에서는 사면 근처에 설치되는 얕은기초의 지지력 보강을 목적으로 strip등의 보강재를 설치할 경우, *'wide slab effect'* 개념등 Huang 및 Binquet-Lee 등이 모형실험등을 통해 제시한 파괴매카니즘 및 Boussinesq 해법 등을 토대로 하여 보강사면에 대한 기초지지력 해석법을 제시하였다. 본 해석법에서는 soil dilatancy 등의 영향에 의한 깊이별 보강재-주변흙 사이의 마찰계수 변화를 함수형태로 표현하여 보강재-주변흙 사이의 상호작용을 부분적으로 고려하였으며, 아울러 본 연구를 통해 제시된 기초지지력 해석법의 적합성 검토를 위해 Huang등이 제시한 모형실험결과와 서로 비교하였다. 이외에도, 설계에 관련된 여러 변수들이 기초지지력에 미치는 영향에 대해서도 분석이 이루어졌다.

Abstract

Recently, foundations of heavy structures such as bridge abutments have been built on slopes or near the crest of slopes at an increasing rate. Because the bearing capacity of such foundations is considerably lower than the bearing capacity of the same soil on a level ground, deep footings such as piles and caissons are often used. However, the costs of such methods are generally very high. One of the new techniques to overcome the problem is to

*[1] Member Associate Professor, Dept. of Civil Eng., Hong-IK Univ.

*[2] Engineer, Dong-Ah Construction Technology & Research.

*[3] Graduate student, Dept. of Civil Eng., Hong-IK Univ.

place reinforcing members such as geosynthetics or metal strips horizontally at some depths beneath the footings. Rational methods of analysis to predict the bearing capacity of footings in reinforced slopes are therefore needed. This paper proposes an analytical method for estimating the increase in bearing capacity gained from the included horizontal strips or ties of tensile reinforcing in the foundation soil below the footing built near the crest of a slope. A failure mechanism, including the concept of 'wide slab effect', adopted in the present study for analyzing the bearing capacity of foundations in reinforced slopes, is established through the observed model test behaviors described by Binquet & Lee and Huang et al., and the Boussinesq solutions. The analytical results are then compared with the experimental data described in the paper by Huang et al. Also in order to properly evaluate the soil-reinforcement interaction, typical pullout test values of the apparent friction coefficient, which usually vary with depths owing to both the increase of the shearing volume and the increase in local stress caused by soil dilatancy, are analyzed and related functionally. Furthermore, analytical parametric studies are carried out to investigate the effect and significance of various pertinent parameters associated with design of reinforced slope foundations.

Keywords : Bearing capacity, Reinforced slope, Slab effect, Friction coefficient

1. INTRODUCTION

Recently, foundations of heavy structures such as bridge abutments have been built on slopes or near the crest of slopes at an increasing rate. Because the bearing capacity of such foundations is considerably lower than the bearing capacity of the same soil on a level ground, deep footings such as piles and caissons are often used. However, the costs of such methods are generally very high. One of the new techniques to overcome the problem is the placement of stiff reinforcing members horizontally at some depths beneath the footings. For natural slopes, this method mainly consists of drilling holes, inserting steel bars and grouting(called 'soil nailing'). For fill embankments, reinforcing members such as geosynthetics or metal strips are placed at prescribed elevations in compacted fill.

This paper proposes an analytical method for estimating the increase in bearing capacity gained from the included horizontal strips or ties of tensile reinforcing in the foundation soil below the footing built near the crest of a slope. A failure mechanism, including the concept of '*wide slab effect*', is established which forms the basis for the bearing capacity analysis of foundations in reinforced slopes. Failure mechanism is examined further by analyses with the FLAC program. The analytical results are then compared with the experimental data. Also in order to properly evaluate the soil-reinforcement interaction, typical pullout test values of the apparent friction coefficient, which usually vary with depths owing to both the increase of the shearing volume and the increase in local stress because of soil

dilatancy, are analyzed and related functionally. Furthermore, analytical parametric studies are carried out to investigate the effect and significance of various pertinent parameters associated with design of reinforced slope foundations.

2. ESTABLISHMENT OF FAILURE MECHANISM

2.1 Failure Mechanism 1

Failure mechanisms of reinforced sandy slopes were investigated by Huang et al.(1990) throughout a series of model loading tests of rough strip footings, and the results are schematically shown in Fig.1.

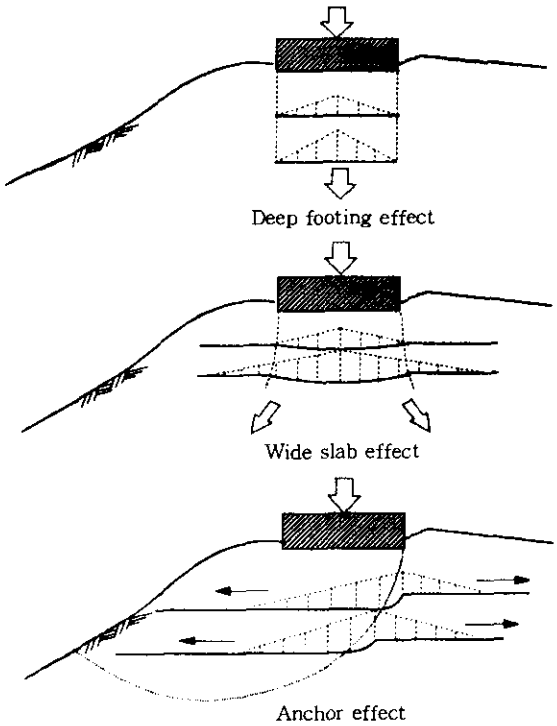

Fig. 1 Observed failure mechanisms of reinforced sandy model slope

According to Huang et al.'s observations of the model tests, the '*anchor effect*', which governs many current design methods, becomes dominant only at very large foundation settlements beyond the peak load. It was therefore concluded by Huang et al. that the applicability of many current design methods to slopes reinforced with relatively stiff reinforcements needs to be re-examined. Fig.1 shows the measured tensile force distributions at the peak footing load reported by Huang et al. It indicates that large tensile forces are mobilized in the reinforcement beneath the footing and, to a lesser extent,

outside the footing width : i.e., the '*deep footing effect*' and '*wide slab effect*' prevail at relatively early stages of loading before the peak footing load. It was also pointed out by Huang et al. that for reinforced level ground, the '*deep footing effect*' is observed in the slope reinforced with a short reinforcement and the '*wide slab effect*' is observed together with the '*deep footing effect*' in the slope reinforced with long reinforcement layers with their length larger than the foundation width. Failure mechanism of reinforced slopes adopted in the present study is due to '*wide slab effect*'. Additional experimental works are required to obtain more precise definitions for this possible failure mechanism.

2.2 Failure Mechanism 2

To evaluate the force developed by the reinforcing ties caused by the applied footing load, it is necessary to formulate a failure hypothesis of the movements and load transfer within the foundation soil.

The location of the shear surface or surfaces through the reinforced sand foundation was not measured precisely in the model tests of level ground carried out by Binquet & Lee (1975-b), and could only be inferred from the location of the broken ties and the ground surface expression after failure. From these observations it was assumed by Binquet & Lee that as the footing load increases, the footing and the soil beneath move down while the soil to the sides moves outward and upward as shown in Fig.2.

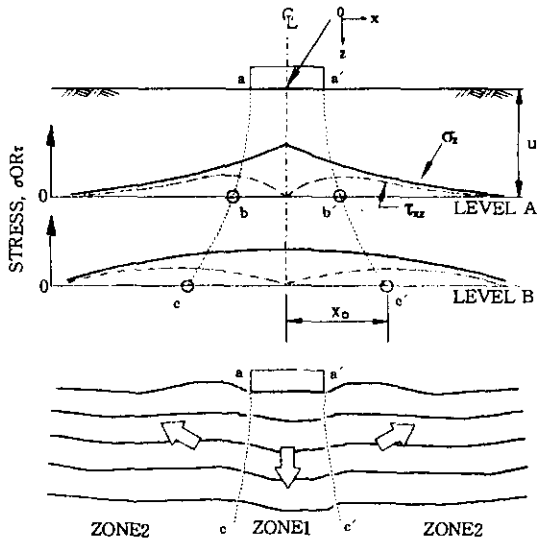

Fig. 2 Failure hypothesis by Binquet & Lee for reinforced level ground

The boundary between the downward moving and outward moving soil was assumed to be defined by the lines a-c and a′−c′ in Fig.2, which are nearly the locus of the points of maximum shear stress $\tau_{xz(max)}$ at every depth z. Note that the locations of many of the

observed tie breaks in the experimental study coincided approximately with these assumed slip surfaces.

To further examine the failure hypothesis proposed by Binquet & Lee(1975-a), an analysis of the shear stresses developed in the slope reinforced with relatively long reinforcing strips is carried out in the present study by using the FLAC(Fast Lagrangian Analysis of Continua) program. Results of an analysis by the FLAC program are illustrated in Fig.3, and parameters used in the analysis are summarized in Table 1. Fig.3 shows that zones of the developed maximum shear stresses, $\tau_{xz\,max}$, match well with the slip surfaces previously described in Fig.2.

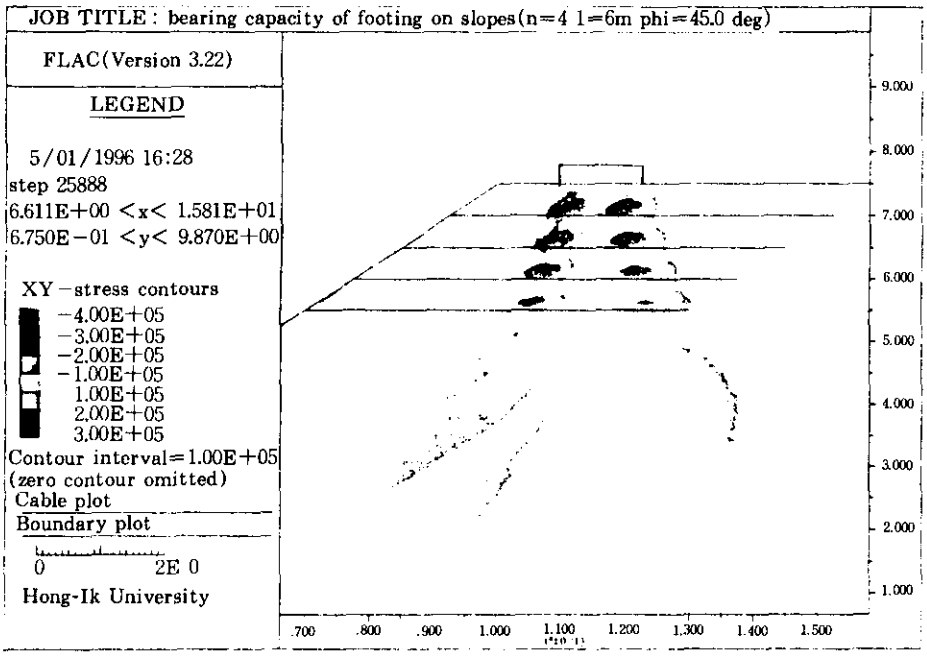

Fig. 3 Contours of developed shear stress by FLAC program analysis

Table 1. Summary of parameters used in the FLAC program

foundation soil	reinforcing strips	
	material	: phosphor bronze
friction angle (ϕ) = 45°	width	: w = 5cm
cohesion (c) = 0.0	thickness	: t = 0.5mm
unit weight (γ_d) = 15.70 KN/m³	yield strength	: f_y = 100GPa
bulk modulus = 13.5 MPa	length	: L = 6m
shear modulus = 29.2 MPa	vertical spacing	: ΔH = 0.5m
slope angle (β) = 30°	position of first layer	: u = ΔH(refer to Fig.2)
	number of layers	: N = 4

From the aforementioned assumptions, the slip is expected to occur along the locus of the points of maximum shear stress, $\tau_{xz\,max}$, at every depth z. The horizontal position of the two symmetrical slip lines, a−c and a′−c′, at any depth z, is defined as x_0 as shown in Fig.4, which may be calculated by differentiating shear stress with respect to x and equating it to zero, i. e.,

$$\frac{d\tau_{xz}}{dx} = 0, \qquad x_0 = \sqrt{\frac{1}{3}(b^2 - z^2 + 2 \cdot \sqrt{z^4 + b^2 z^2 + b^4})} \tag{1}$$

where,

$b = \frac{B}{2}$

B = foundation width

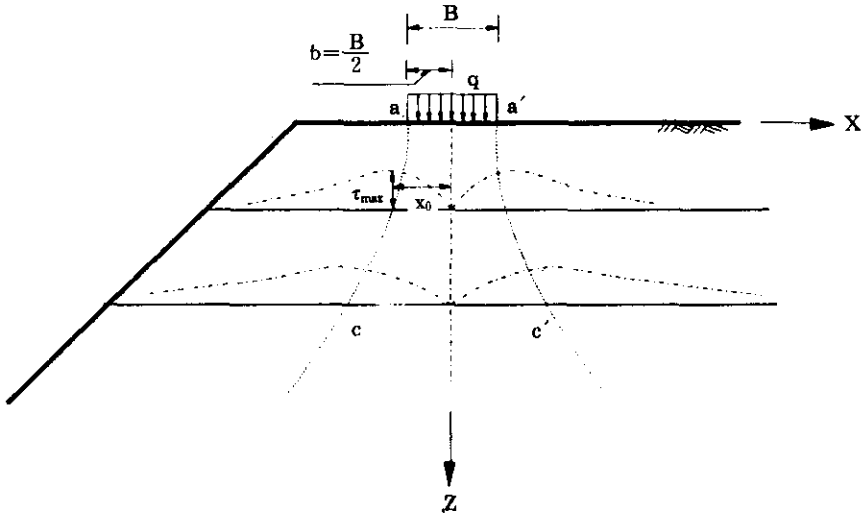

Fig. 4 Shear stress distribution caused by the applied footing stress q

At the same time, the values of the shear stresses and normal stresses at any location defined by x and z coordinates may also be calculated based on the Boussinesq solutions.

Fig.5 shows the case where a uniform vertical stress of q per unit area acts on a flexible infinite strip on the surface of a semi-infinite elastic mass. The total increases in vertical stress, σ_z, and shear stress, τ_{xz}, caused by the loaded strip at N can be determined as

$$\sigma_z = \frac{q}{\pi}\left[\tan^{-1}\left(\frac{x+b}{z}\right) - \tan^{-1}\left(\frac{x-b}{z}\right) - \frac{2bz(x^2 - z^2 - b^2)}{(x^2+z^2+b^2)^2 - 4b^2x^2}\right] \tag{2}$$

$$\tau_{xz} = \frac{4bqxz^2}{\pi[(x^2+z^2-b^2)^2 + 4b^2z^2]} \tag{3}$$

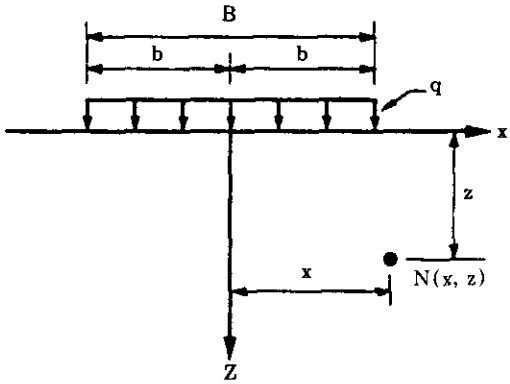

Fig. 5 Schematics of Boussinesq solutions

The horizontal variation of these stress components at different levels takes the form shown in Fig.2. It is assumed that these stresses are independent of whether the foundation soil is reinforced or not. Thus, for $q=q_o$, identical values of stresses are obtained at the same locations in the reinforced or the unreinforced foundation soil.

3. METHOD OF BEARING CAPACITY ANALYSIS

As shown in Fig. 6, the increase in bearing capacity of a foundation in a reinforced slope should be evaluated on the basis of the length of reinforcement.

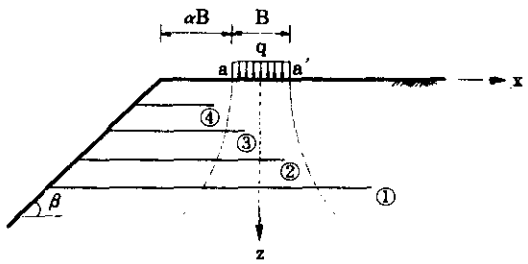

Fig. 6 Classification of reinforcement installation type

Let the length of reinforcing strip from the center of a foundation to the slope be L_s. Also for Case Ⅰ and Case Ⅱ, let the length of reinforcing strip from the center of a foundation to the opposite side of the slope be L_g. The analysis procedure can then be classified into the following four cases :

① Case Ⅰ : $(L>L_s+x_o)$

② Case Ⅱ : $(L_s<L<L_s+x_o)$

③ Case Ⅲ : $(L_s - x_o < L < L_s)$

④ Case Ⅳ : $(L < L_s - x_o)$

where,

$$L_s = \frac{B}{2} + \alpha B + \frac{z}{\tan\beta}$$

αB = horizontal distance from the crest of the reinforced slope to the foundation

$L_g = L - L_s$

① Case Ⅰ $(L > L_s + x_o)$

The vertical normal forces(F_1, F_1', F_2 and F_2') and the vertical shear forces(S_1 and S_1') acting on the boundaries of the element cdc'd' in the unreinforced soil are described in Fig. 7. These forces are due to the normal and shear stresses at the depth z caused by the applied bearing pressure q_o on the footing.

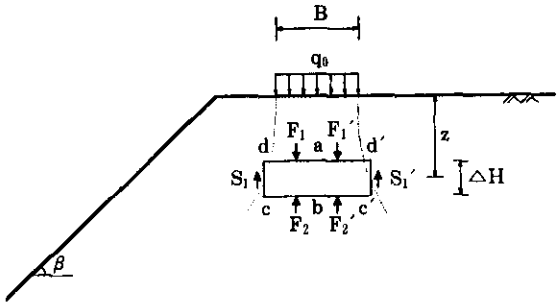

Fig. 7 **Components of forces in the unreinforced soil**

The magnitude of these forces may be readily calculated by integrating the appropriate stresses over the appropriate areas as follows.

$$F_1 = F_1'$$

$$= \int_0^{x_o} \sigma_z\,(q_o, x, z)dx$$

$$= \frac{q_0}{\pi}\left[(x_o+b)\tan^{-1}\left(\frac{x_o+b}{z}\right) - (x_o-b)\tan^{-1}\left(\frac{x_o-b}{z}\right)\right]$$

$$= J \cdot q_o \cdot B \qquad (4)$$

where, $J = \frac{1}{\pi B}\left[(x_o+b)\tan^{-1}\left(\frac{x_o+b}{z}\right) - (x_o-b)\tan^{-1}\left(\frac{x_o-b}{z}\right)\right]$

$$S_1 = S_1'$$

$$= \tau_{xz}(q_o, x_o, z) \cdot \Delta H$$

$$= \frac{4bq_o x_o z^2}{\pi[(x^2+z^2-b^2)^2+4b^2z^2]} \cdot \Delta H$$

$$= I \cdot q_o \cdot \Delta H \qquad (5)$$

where, $I = \dfrac{4bx_0z^2}{\pi[(x^2+z^2-b^2)^2+4b^2z^2]}$ (6)

Equilibrium of the element cdc′d′ in the unreinforced soil may be expressed as

$$(F_3+F_3')-(F_2+F_2')-(S_1+S_1')=0 \tag{7}$$

Similar to the unreinforced soil case, the forces F_3, F_2', S_2, and S_2' for the reinforced soil as described in Fig.8 can be expressed as

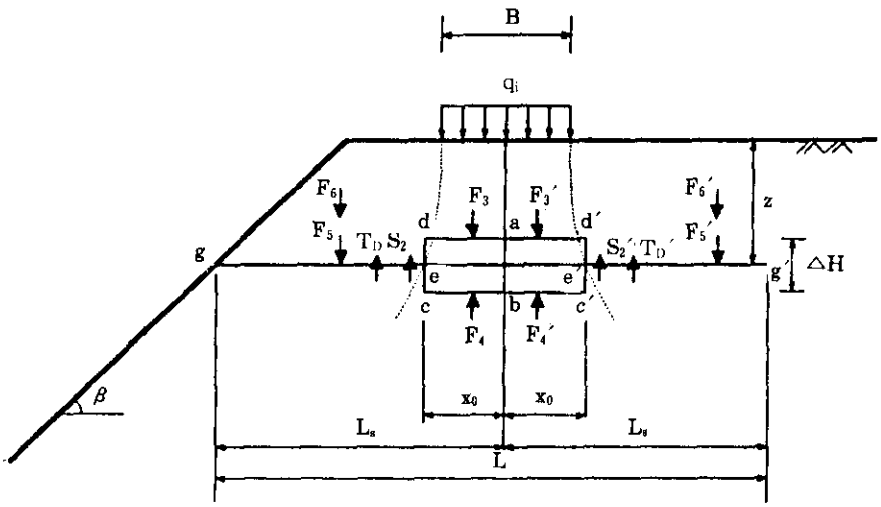

Fig. 8 Components of forces in the reinforced soil(Case I)

$$\begin{aligned} F_3 &= F_3' \\ &= \int_0^{x_0} \sigma_z(q_i, x, z)dx \\ &= J \cdot q_i \cdot B \end{aligned} \tag{8}$$

$$\begin{aligned} S_2 &= S_2' \\ &= \tau_{xz}(q_i, x_0, z) \cdot \Delta H \\ &= I \cdot q_i \cdot \Delta H \end{aligned} \tag{9}$$

For the special case of a single layer of reinforcing in the foundation (N=1), equilibrium of the element cdc′d′ as shown in Fig. 8, may be expressed as

$$(F_3+F_3')-(F_4+F_4')-(S_2+S_2')-(T_D+T_D') = 0 \tag{10}$$

in which T_D+T_D' represents the tensile force developed in the reinforcements.

The analysis proceeds by assuming that the forces are evaluated for a given foundation width B and settlement s for a foundation on unreinforced soil and on reinforced soil. Based on this assumption, it follows that the upward forces on the soil below the element cdc′d′ are the same for the unreinforced and the reinforced foundation :

$$F_2+F_2' = F_4+F_4' \tag{11}$$

Rearrangement of Eqs. (7), (10) and (11) gives the expression for the tensile force developed in reinforcing strips as follows :

$$T_D+T_D' = 2(J \cdot B-I \cdot \Delta H)(q_i-q_o) \quad (12)$$

where ΔH = vertical spacing between reinforcing strips.

The mechanism by which the strip force T_D' is developed requires additional assumptions to the basic failure hypothesis. It is pragmatically assumed that as the central zone of soil moves down with respect to the outer zone along the slip surface a′−c′, it drags the strips along with it as shown in Fig.9.

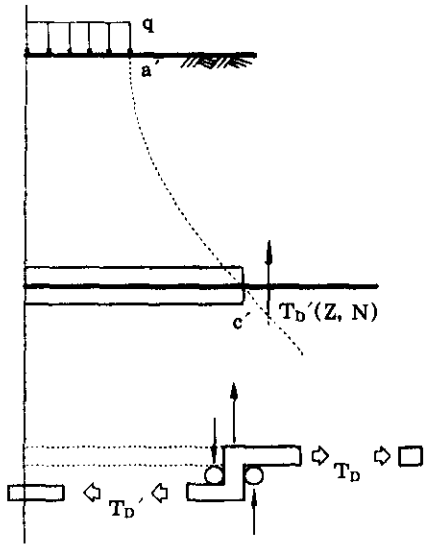

Fig. 9 Basic failure hypothesis

At the slip surface the strips are assumed to undergo two right angle bends around two frictionless rollers. At the surface the strip resistance T_D' is a vertically acting tensile force.

Elsewhere, on either side the tie resistance acts horizontally along the axis of the strip and the forces are transferred into the soil by means of soil-strip friction. For lack of definitive data, it is arbitrarily assumed that the strip force per layer varies inversely with the number of layers N in the foundation. Thus

$$T_{D(N)}+T_{D(N)}' = \frac{2}{N}(J \cdot B-I \cdot \Delta H)(q_i-q_o) \quad (13)$$

Calculation of strip pullout resistance requires evaluation of the total vertical normal forces F_5 and F_5', acting on the lengths eg and e′g′ of the strip outside the assumed shear surface(Figs.7 and 8) :

$$F_5 = LDR \int_{x_0}^{L_5} \sigma_z(q_i, x, z)dx$$

$$= \mathrm{LDR}\,\frac{q_i}{\pi}\Big[\,(L_s+b)\tan^{-1}\left(\frac{L_s+b}{z}\right)-(L_s-b)\tan^{-1}\left(\frac{L_s-b}{z}\right)$$

$$-(x_o+b)\tan^{-1}\left(\frac{x_o+b}{z}\right)-(x_o-b)\tan^{-1}\left(\frac{x_o-b}{z}\right)\Big]$$

$$= \mathrm{LDR}\cdot M\cdot q_i\cdot B \tag{14}$$

$$M = \frac{1}{\pi B}\Big[\,(L_s+b)\tan^{-1}\left(\frac{L_s+b}{z}\right)-(L_s-b)\tan^{-1}\left(\frac{L_s-b}{z}\right)$$

$$-(x_o+b)\tan^{-1}\left(\frac{x_o+b}{z}\right)-(x_o-b)\tan^{-1}\left(\frac{x_o-b}{z}\right)\Big] \tag{15}$$

$$F_5' = \mathrm{LDR}\int_{x_o}^{L_g}\sigma_z(q_i,\,x,\,z)\,dx$$

$$= \mathrm{LDR}\cdot M'\cdot q_i\cdot B \tag{16}$$

$$M' = \frac{1}{\pi B}\Big[\,(L_g+b)\tan^{-1}\left(\frac{L_g+b}{z}\right)-(L_g-b)\tan^{-1}\left(\frac{L_g-b}{z}\right)$$

$$-(x_o+b)\tan^{-1}\left(\frac{x_o+b}{z}\right)-(x_o-b)\tan^{-1}\left(\frac{x_o-b}{z}\right)\Big] \tag{17}$$

where, LDR = linear density of reinforcement (= $w\cdot N_R$)

w = width of a single strip

N_R = number of reinforcing strips per unit length of the foundation.

The total vertical normal force F_{Nt} on the strip over the lengths eg and e′g′ can be calculated as

$$F_{Nt} = F_5+F_5'+F_6+F_6'$$

$$= F_5+F_5'+\mathrm{LDR}(W_1+W') \tag{18}$$

in which W_1 and W_1' are the normal overburden forces on the strip over the length eg and e′g′ respectively.

Combining Eqs. (14), (16) and (18) leads to an expression for strip pullout frictional resistance, T_f+T_f', per unit length of the foundation and depth z :

$$T_f+T_f' = 2f\,\mathrm{LDR}\,\{(M+M')Bq_i+W_1+W'+\eta\frac{c}{f}(L-2x_o)\} \tag{19}$$

where, f = apparent friction coefficient

c = cohesion

η = influence factor of cohesion

The increment of bearing capacity, Δq_i, for each of the reinforcing layer depths is determined as follows :

$$\Delta q_i = q_i-q_o \tag{20}$$

in which q_i is calculated by equating Eq. (13) to Eq. (19). The expression for q_i is given below.

$$q_i = \frac{q_o(J\cdot B-I\cdot\Delta H)+N\cdot f\cdot \mathrm{LDR}\cdot\{W_1+W'+c(L-2x_o)/f\}}{J\cdot B-I\cdot\Delta H-N\cdot f\cdot \mathrm{LDR}\cdot(M+M')B} \tag{21}$$

② Case Ⅱ ($L_s<L<L_s+x_o$)

In Case Ⅱ ($L_s<L<L_s+x_o$, Fig. 10), no strip force is expected to develop in the opposite side of the slope.

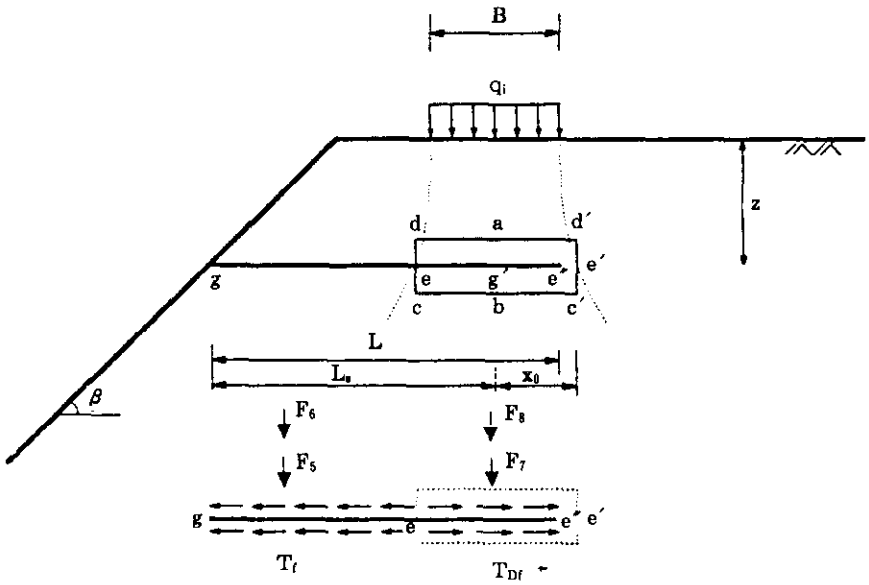

Fig. 10 Components of forces in the reinforced soil(Case Ⅱ)

The strip tensile force, $T_{D(N)}$, developed in any layer of reinforcements in the slope side is thus

$$T_{D(N)} = \frac{1}{N}(J \cdot B - I \cdot \Delta H)(q_i - q_o) \tag{22}$$

Strip pullout frictional resistance, T_f, on the length, eg, of the strip is calculated as

$$T_f = 2 \cdot f \cdot LDR \{M \cdot B \cdot q_i + W_1 + \eta c(L_s - x_o)/f\} \tag{23}$$

If the entire length of the strip is L_s+x_o, increased bearing capacity, $q_{i(e)}$, can be calculated as

$$q_{i(e)} = \frac{q_o(J \cdot B - I \cdot \Delta H) + 2 \cdot N \cdot f\, LDR\{W_1 + \eta c(L_s - x_o)/f\}}{J \cdot B - I \cdot \Delta H - 2 \cdot N \cdot f \cdot LDR \cdot M \cdot B} \tag{24}$$

The vertical force F_7 as shown in Fig. 10 is caused by the vertical stresses over the length ee″ imposed by the applied bearing pressure q_i on the footing. And the vertical force F_8 is due to the normal overburden force on the length ee″ of the strip. The expressions for F_7 and F_8 are given below.

$$F_7 = LDR\left(\int_0^{L_g} \sigma_z(q_i, x, z)dx + \int_0^{x_o} \sigma_z(q_i, x, z)dx\right)$$

$$= LDR\,\frac{q_i}{\pi}\left[\,(x_o+b)\tan^{-1}\left(\frac{x_o+b}{z}\right) - (x_o-b)\tan^{-1}\left(\frac{x_o-b}{z}\right)\right.$$

$$+(L_g+b)\tan^{-1}\left(\frac{L_g+b}{z}\right)-(L_g-b)\tan^{-1}\left(\frac{L_g-b}{z}\right)\Big]$$
$$= LDR\cdot(J+J')\cdot B\cdot q_i \tag{25}$$

where

$$J' = \frac{\int_0^{L_g}\sigma_z(q_i, x, z)dx}{B\cdot q_i}$$
$$= \frac{1}{\pi\cdot B}\left[(L_g+b)\tan^{-1}\left(\frac{L_g+b}{z}\right)-(L_g-b)\tan^{-1}\left(\frac{L_g-b}{z}\right)\right] \tag{26}$$

and $F_8 = LDR\cdot W_2$ (27)

In Case Ⅱ the entire length of the strip, L, can vary in the following range : $L_s<L<L_s+x_o$. Using similar procedures applied to the Case Ⅰ and assuming proportional variation regarding the mobilized frictional resistance on the length, ee′, of the reinforcing strip, the expression for the increment of bearing capacity, Δq_i, for each of the reinforcing layer depths is determined as

$$\Delta q_i = \frac{(J+J')B\cdot q_o+W_2+\eta c(L_g+x_o)/f}{2\cdot J\cdot B\cdot q_{i(e)}+W_{i(e)}+2\eta c x_o/f-(J+J')B\cdot\Delta q_{i(e)}}\cdot\Delta q_{i(e)} \tag{28}$$

in which $W_{i(e)}$ and W_2 are the normal overburden forces on the strip over the length ee′ and ee″ respectively.

(3) Case Ⅲ $(L_s-x_o<L<L_s)$

The vertical forces F_7' and F_8' as shown in Fig.11 are determined through similar procedures applied to Case Ⅱ and the resulting expressions are given below.

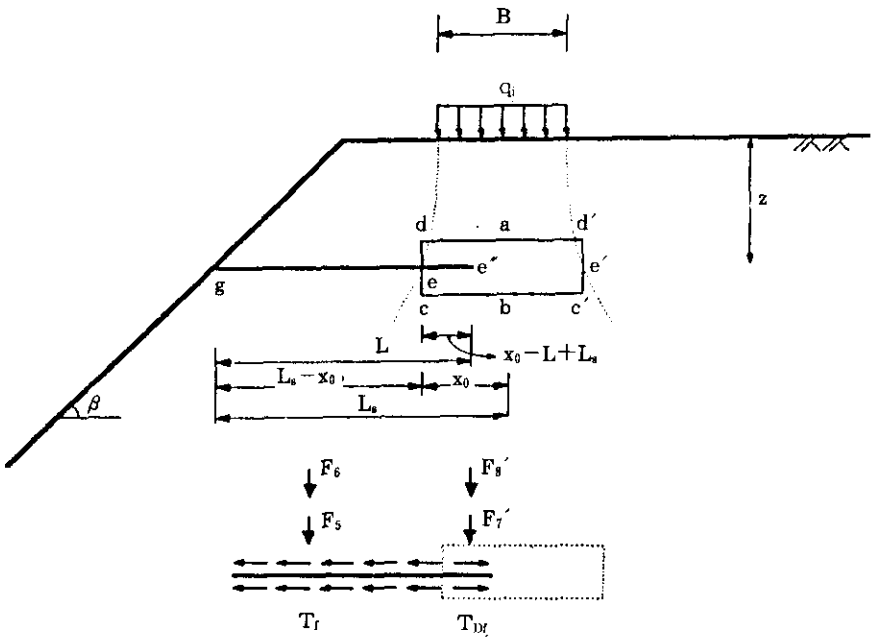

Fig. 11 Components of forces in the reinforced soil(Case Ⅲ)

$$F_7' = LDR\int_{L_x}^{x_0} \sigma_z(q_i, x, z)dx$$

$$= LDR\frac{q_i}{\pi}\Big[(x_0+b)\tan^{-1}\left(\frac{x_0+b}{z}\right)-(x_0-b)\tan^{-1}\left(\frac{x_0-b}{z}\right)$$

$$-(L_x+b)\tan^{-1}\left(\frac{L_x+b}{z}\right)-(L_x-b)\tan^{-1}\left(\frac{L_x-b}{z}\right)\Big]$$

$$= LDR \cdot K \cdot q_i \cdot B \tag{29}$$

where

$$K = \frac{1}{\pi B}\Big[(x_0+b)\tan^{-1}\left(\frac{x_0+b}{z}\right)-(x_0-b)\tan^{-1}\left(\frac{x_0-b}{z}\right)$$

$$-(L_x+b)\tan^{-1}\left(\frac{L_x+b}{z}\right)+(L_x-b)\tan^{-1}\left(\frac{L_x-b}{z}\right)\Big]$$

and $F_8' = LDR \cdot W_2$ (30)

By using similar procedures applied to Case Ⅱ the expression for the increment of bearing capacity, Δq_i, for each of the reinforcing layer depths is determined as

$$\Delta q_i = \frac{K \cdot B \cdot q_0+W_2+\eta c(x_0+L-L_s)/f}{2 \cdot J \cdot B \cdot q_{i(e)}+W_{(e)}+2\eta c x_0/f-K \cdot B\Delta q_{i(e)}} \cdot \Delta q_{i(e)} \tag{31}$$

④ Case Ⅳ ($L<L_s-x_0$)

In Case Ⅳ ($L<L_s-x_0$, refer to Fig.6), no reinforcing effects are expected because the reinforcing strip is placed outside the assumed failure surface.

3.1 Increased Total Bearing Capacity

The total bearing capacity q in the reinforced soil can be determined as the sum of bearing capacity increments, Δq_i, in each layer of reinforcing strips.

$$q = q_0+\sum_{i=1}^{N}\Delta q_i \tag{32}$$

3.2 Internal Stability

The developed tensile force, $T_{D(N)}+T_{D(N)}'$, in any layer of reinforcement should satisfy the following internal stability condition.

$$T_{D(N)}+T_{D(N)}' \le \left(\frac{R_y}{FS_y}, \frac{T_f+T_f'}{FS_f}\right) \tag{33}$$

in which R_y = the yield strength of the reinforcement, T_f+T_f' = the frictional pullout resistance of the reinforcement layer, FS_y = the factor of safety against yield failure, and FS_f = the factor of safety against pullout failure.

The yield strength of the reinforcement may be calculated from

$$R_y = \frac{w \cdot N_R \cdot t \cdot f_y}{FS_y} = \frac{LDR \cdot t \cdot f_y}{FS_y} \tag{34}$$

in which w = the width of a single reinforcement, t=the thickness of a single reinforcement, N_R=the number of reinforcement layers per unit length of a foundation, and f_y=the yield stress of the reinforcement.

The term $w \cdot N_R$ represents the total width of reinforcement strips per unit length of a foundation and it may be conveniently expressed as the linear density of reinforcement (LDR) as

$$LDR = w \cdot N_R \tag{35}$$

3.3 Soil-Reinforcement Interaction

In dense granular soils, values of the apparent friction coefficient f between the strip and surrounding soil are usually significantly greater than the values obtained from direct shear tests. This is mainly because dense granular soil in the vicinity of the reinforcements tend to increase the volume, i.e., dilate during shear. This positive volume change is restrained by the surrounding soil. When ribbed strips are used, the ribs cause the shearing zone of soil to increase in size. Both the increase in the shearing volume, and the increase in local stress caused by soil dilatancy, result in an increase in the apparent friction coefficient, f, which is defined as a ratio :

$$f = \frac{\tau_{ave}}{\sigma_v} = \frac{T}{2bL\sigma_v} \tag{36}$$

where τ_{ave}=the average shear stress along the reinforcement, σ_v=the overburden stress, T=the applied pullout force, t=the width of the reinforcement, and L=the length of the reinforcement.

Pullout tests on reinforcements located in actual structures, as well as laboratory studies

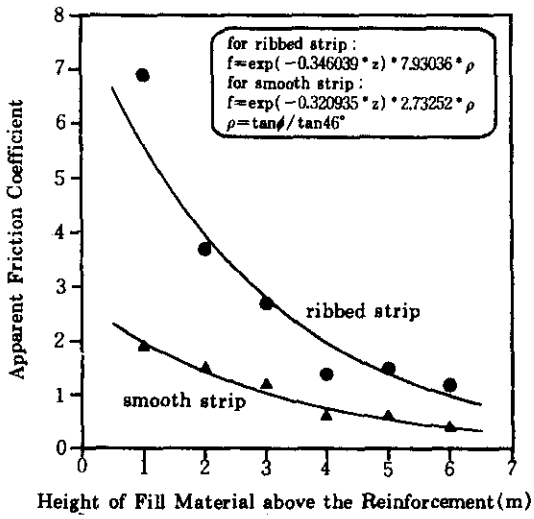

Fig. 12 Variation of f with height of fill material above the reinforcement

using dense sands, show that the value of the apparent friction coefficient decreases when the vertical overburden stress increases. This phenomenon is more pronounced in the case of ribbed reinforcements than in the case of smooth reinforcements.

In order to properly reflect the influence of the vertical overburden stress, pullout test values of the apparent friction coefficient, f, on gravel sand(γ=21KN/m^3, ϕ=46°) reported by Schlosser & Elias(1978) are analyzed in the present study by regression ; and for the ribbed reinforcement and the smooth reinforcement functional expressions for the friction coefficient f are given as shown in Fig.12.

4. COMPARISON WITH MODEL TEST RESULTS

A series of model tests were conducted by Huang et al.(1990) to investigate the fundamental behavior of reinforced slopes of dense Toyoura Sand(γ=15.5KN/m^3, ϕ=45°). In model tests a rigid, rough 10 cm wide strip footing as shown in Fig.13 was loaded at a constant vertical displacement rate of 0.15 mm/sec. During the loading the footing was free to displace laterally and to rotate.

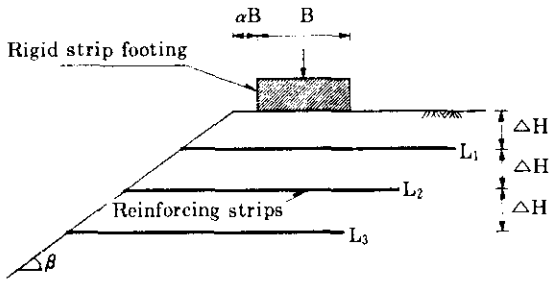

Fig. 13 Schematics of reinforced slope model test

The reinforcing strips, 0.5 mm thick, 3mm wide, and 0.166~0.4m long, were made of phosphor bronze. The yielding strength of these strips, f_y, was 1.7×10^5KN/m^2. Three layers of reinforcing strips with vertical spacing, ΔH, of 0.03 or 0.05 m were used for tests.

Measured values of the bearing capacity for the three tests conducted by Huang et al. (1990) are compared with those calculated by the proposed analytical method. In the analysis, adopted values of the factors of safety, FS_γ and FS_ϕ, are 3.0, and also functional relationship of the smooth reinforcement case given in Fig.12 is used.

The results of comparisons with detailed descriptions of these tests are summarized in Table 2. Overall, the proposed analytical method of analysis gives very comparable results, generally within 6~12% of the measured bearing capacity.

Table 2. Bearing capacity comparisons with model test results

Test No.	vertical spacing ΔH(m)	length of reinforcing strips L_i(m)	bearing capacity q(KN/m²)	
			measured by Huang et al.	calculated by presently proposed method
No.4	0.03	$L_1 = L_2 = L_3 = 0.4$	89.1	82.2
No.6	0.05	$L_1 = L_2 = L_3 = 0.4$	112.7	126.1
No.8	0.03	$L_1 = 0.166$ $L_2 = 0.202$ $L_3 = 0.238$	45.5	42.8

5. PARAMETRIC STUDY

Analytical parametric studies are carried out to investigate the effect and significance of various pertinent parameters on the bearing capacity of foundations in reinforced slopes. The parameters selected for these parametric studies are the length of reinforcing strip(L), the distance from the crest of a slope to the foundation($\alpha \cdot B$), the slope angle(β), the linear density of reinforcement(LDR), the number of reinforcing strip layers(N), and the distance from the foundation to the first layer of reinforcing strip(u). Detailed values of the selected parameters for these parametric studies are summarized in Table 3.

Table 3. Summary of values of parameters used in parametric studies

constants	variables
$\phi = 30°$	$\Delta H = 0.2 \sim 1.0$m
$c = 0$	$L = 2 \sim 5$m
$\gamma = 15$KN/m³	$\alpha = 0 \sim 2.5$
$w = 0.1$m	$\beta = 20 \sim 40°$
$t = 0.005$ m	LDR = 10~30%
$B = 1$m	$N = 2 \sim 4$
	$u = 0.2 \sim 0.5$m

In these parametric studies, the phrase Bearing Capacity Ratio(BCR) is adopted for convenience in expressing and evaluating the reinforcement effects as

$$BCR = q/q_o \tag{37}$$

in which q and q_o are, respectively, the bearing capacity for the reinforced and the unreinforced soil at any desired vertical foundation settlement before the foundation actually fails with very large settlements. In the present study, the bearing capacity equation presented by Kusakabe et al. (1981) is used to evaluate q_o, i.e.,

$$q_o = cN_c + \frac{1}{2}\gamma BN_\gamma \tag{38}$$

in which N_c and N_γ are bearing capacity factors.

Note also that the type and size of reinforcement, and the foundation width(B) and corresponding soil properties are kept constant in these studies.

By analyzing the results of these parametric studies as illustrated in Figs. 14~19, the following observations are drawn.

- Longer reinforcement gives higher BCR value(Fig.14).

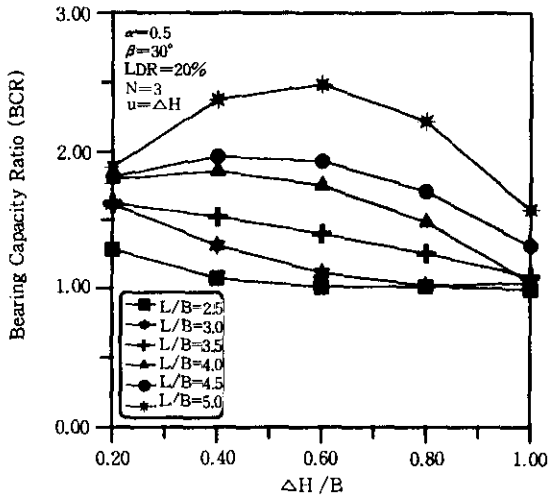

Fig. 14 Variation of BCR with △H/B and L

- As the value of α decreases, i.e., as the horizontal distance from the crest of the reinforced slope to the foundation becomes shorter, the reinforcing effect gradually increases(Fig.15).

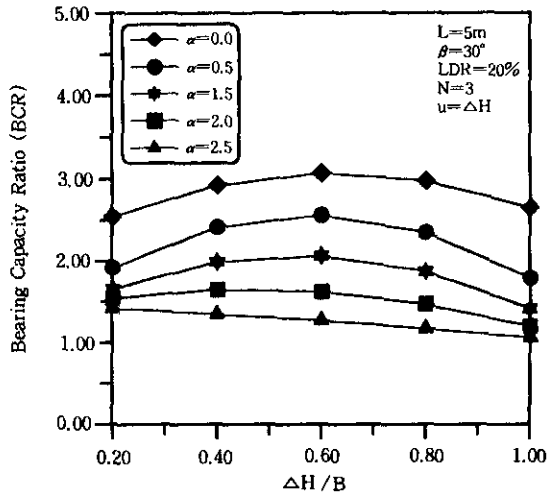

Fig. 15 Variation of BCR with △H/B and α

• The BCR value gradually increases as the reinforced slope becomes steeper(Fig.16).

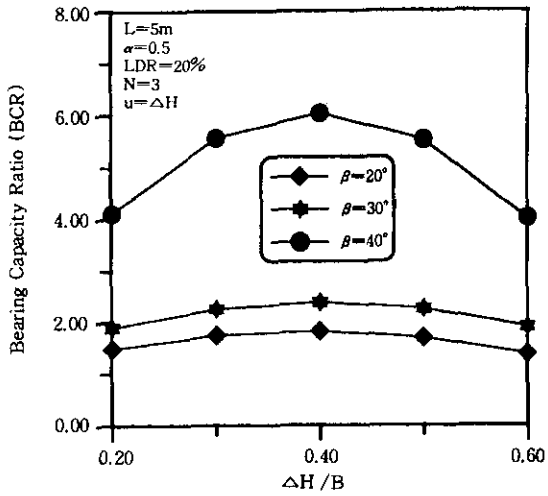

Fig. 16 Variation of BCR with $\Delta H/B$ and β

• The BCR value increases by about 60~90% with increasing LDR for cases of $\Delta H/B$ less than 0.6. However, for cases of $\Delta H/B$ greater than 0.6, the BCR values tend to decrease. For the case where LDR=30%, the BCR value increases more rapidly for values of $\Delta H/B$ between 0.2 and 0.4(Fig.17).

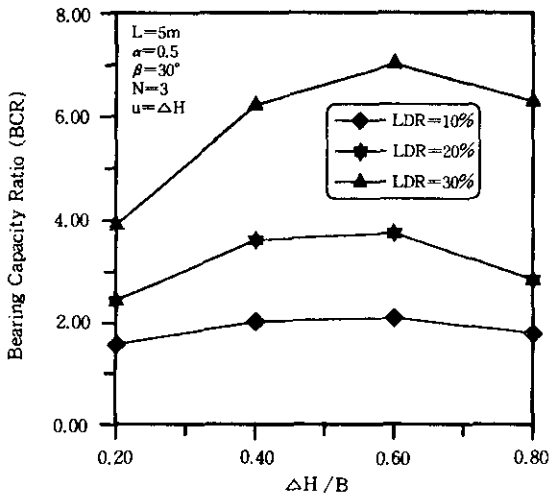

Fig. 17 Variation of BCR with $\Delta H/B$ and LDR

• In general the BCR value increases when the number of reinforcing strip layers increase. The increasing rate of the BCR value, however, tends to gradually decrease when the values of ΔH/B increase. For the case where N=2, the BCR values remain more or less constant irrespective of the values of ΔH/B(Fig.18).

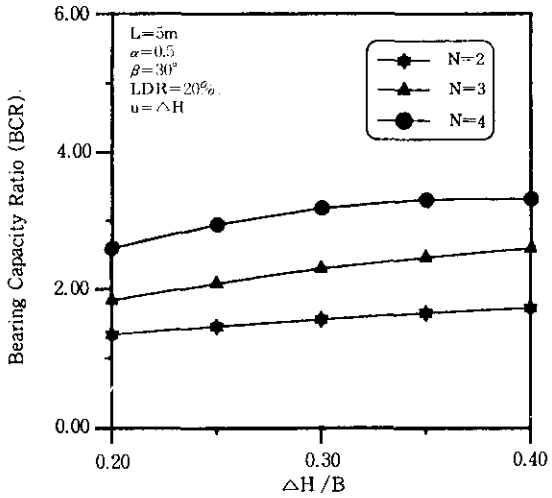

Fig. 18 Variation of BCR with △H/B and N

• Value of ΔH/B at which maximum BCR value is expected is in the range between 0.4~0.5. The value of ΔH/B at which maximum BCR value is expected is generally unaffected by u/B which defines the position of the first reinforcing strip layer(Fig.19).

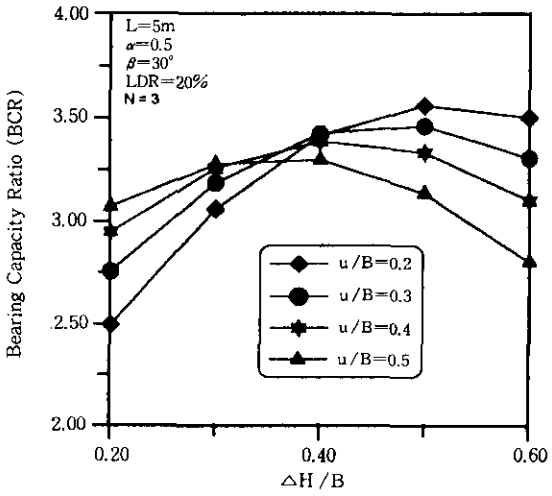

Fig. 19 Variation of BCR with △H/B and u

6. CONCLUSIONS

In the present study an analytical method is presented for evaluating bearing capacity of a foundation adjacent to a slope reinforced with horizontal layers of strips or ties with relatively high tensile strength. The validity of the proposed analytical method is checked by comparing the results with data from experimental model tests described in the paper by Huang et al. The comparison in general shows good agreement with measured values of bearing capacity. A failure mechanism, including the concept of '*wide slab effect*', adopted in the present study for analyzing the bearing capacity of foundations in reinforced slopes, is established through the observed model test behaviors described by Binquet & Lee and Huang et al., and the Boussinesq solutions. The FLAC program is used to further examine the failure mechanism. In order to properly take into account both the increase in the shearing volume and the increase in local stress caused by soil dilatancy, typical pullout test values of the apparent friction coefficient reported by and Schlosser & Elias are analyzed in the present study by regression, and functionally related. Using the proposed analytical method, parametric studies are also carried out to investigate the effect and significance of various pertinent parameters considered important. The observations drawn from these parametric studies may provide useful informations in designing reinforced slope foundations. Further experimental studies are, however, necessary to verify these analytical findings.

ACKNOWLEDGEMENTS

Financial support for this study is provided the Hong-Ik University(1994~1995), and this support is gratefully acknowledged.

REFERENCES

1. Binquet, J., and Lee, K.L. (1975-a) "Bearing Capacity Analysis of Reinforced Earth Slabs," ASCE, *Journal of Geotechnical Engineering*, Vol. 101, No. GT12, pp.1257~1276.
2. Binquet, J., and Lee, K.L. (1975-b) "Bearing Capacity Tests on Reinforced Earth Slabs," ASCE, *Journal of Geotechnical Engineering*, Vol. 101, No. GT12, pp.1241~1255.
3. Huang, C.C., Tatsuoka, F. and Sato, Y. (1990) "Bearing Capacity of Footings in Sandy Slopes," *10th Southeast Asian Geotechnical Conference*, Taipei, pp.163~168.
4. Kusakabe, O., Kimura, T. and Yamaguchi, H. (1981) "Bearing Capacity of Slopes under Strip Loads on the Top Surface," *JSSMFE*, Vol. 21 No. 4 pp.29~40.
5. Schlosser, F. and Elias, V. (1978) "Friction in Reinforced Earth," *Proc. ASCE Symp. of Earth Reinforcement*, Pittsburgh, pp.735~762.

(received on Apr. 25, 1996)